Bio-Optical Characterization And Ecological Plasticity Of The Hooghly-Matla Estuarine Ecoregion - An ISRO-Sponsored Study On The Impact Of Cyclone Remal On The Optically Complex Shallow Waters Of Northwestern Bay Of Bengal

Dr. Abhishek Mukherjee[1], Prof. Tarun Kumar De[2], Dr. Anurag Gupta[3]

[1, 2] Department of Marine Science, University of Calcutta; 35 Ballygunge Circular Road, Kolkata – 700019, West Bengal, India

[3] Marine Ecosystem Division, Biological and Planetary Science Group (BPSG-EPSA), Space Applications Centre, Ahmedabad - 380015, Gujarat, India

Abstract- *The present study was aimed at assessing the impact of tropical cyclonic storms on mangrove dominated vertically well-mixed estuaries. The landfall of Cyclone Remal over an area that is predominantly the Sundarban straddling Hooghly-Matla estuarine complex provided with such an opportunity since it was already under environmental monitoring at the time. A considerable array of relevant variables was chosen for the study encompassing meteorological, physicochemical, as well as biological sections of the ecosystem. The observed values of mean meteorological and physical variables were not much different in the wake of the storm after a few weeks than what was recorded prior to the storm. Dissolved Nitrates, Phosphates, and Silicates were relatively higher following the storm, but not to the anticipated extent. This had triggered an influx of stenohaline phytoplankton owing to lingering shifts in salinity and pH following the storm, conducive enough for the species. This change was not exclusive of the euryhaline species but was sufficient to modify the diversity index of the population. It was also reflected on Chl a and TSM data, corroborated by both in situ and OCM 3 satellite generated readings, in spite of the population density being not too dissimilar to pre storm state. The effect of the storm was observed in CDOM contents as well but due to the unique nature of the estuary itself, it was already observed bordering on pre storm data even only a few weeks later.*

Keywords- Bay of Bengal, Cyclone, Hooghly Estuary, Sundarban Mangrove, Water Quality

I. INTRODUCTION

A cyclone brings with it a large array of changes that can be either ephemeral or far reaching depending on the nature of the water body being subjected to its disruptive influences (Chaco and Jayaram, 2022; Madeiros, 2022; Devi et al, 2021; Mukherjee et al, 2013; Mukherjee et al., 2012). Well mixed estuaries and large mesotidal rivers bounce back from the changes within a rather short time span once the actual period of turbulence gets over with (Wang et al., 2010; Bonvillain et al., 2011), as compared to the ones which are subjected to dominance from either the river or the sea (Xu et al., 2020; Zhang et al., 2014). Episodic natural calamities, such as major storms in the form of hurricanes/cyclones/typhoons etc. can and do alter the nutrient regime within a very short period of time owing to the immense amount of terrestrial runoffs as well as resuspension of deep-seated sediment beds within the water column, leading to rapid increase in inorganic and organic compounds which eventuate in a spike in primary productivity (Mukherjee et al., 2013; Shiah et al., 2000; McDiffett et al., 1989); excessive nutrients also trigger massive algal blooms which inevitably lead to localized hypoxia (Zhang et al. 2014; Paerl and Paul, 2012), affecting the aquatic life very adversely more often than naught (Zhang et al. 2022; Mukherjee et al, 2012) The ameliorative effects from any one of them takes longer to gain traction in the absence of adequate counteractive actions by either of the two masses of water (viz. Salt wedge estuaries, or Fjords etc. where River and the Sea play the dominant role respectively).

The waters of North West Bay of Bengal constitute a well-mixed estuary, the Hooghly-Matlah deltaic ecoregions, where freshwater and marine influences equally shape and reshape the ecosystem (De et al., 2021; Mukhopadhyay et al, 2006) in addition to a considerable tract of bordering mangrove forests, the Sundarbans, all of which contribute to assign a specific set of characteristics to the environment. The estuary, positive and mixohaline (Sadhuram et al., 2005), boasts an average depth of the shallow estuary is 6 meters. Intense tidal mixing and shallow depths render the Hooghly

estuary well-mixed and vertically consistent all year long, with the exception of a brief window during the June–September southwest monsoon season when the estuary becomes somewhat stratified as a result of increased freshwater discharge. The existence of islands, considerable tidal changes, irregular shoreline geometry, and navigational channels divided by shallow zones all contribute to the flow complexity (Biswas, 1985). It is also prone to many significant cyclonic circulations (leading to powerful cyclones) which are either formed in or make landfall through these waters, thereby wreaking havoc to the entire ecosystem each year, with at least one of them being equivalent to Category 4 or 5 tropical hurricanes (https://severeweather.wmo.int/index.html).

'Remal' was such a cyclone which made landfall on 26th of May, 2024 near the Sundarbans as 'Severe Cyclonic Storm'(IMD), equivalent to a Category 1 Hurricane, with a sustained wind speed between 100 – 135 Kmh^{-1} (~65-80 mph) and a gusts of over 140 Kmh^{-1} (~85 mph) [Lowest registered pressure: 978 hPa (mbar); 28.88 inHg]. The Indian Meteorological Department had designated it as BOB 0, while the Joint Typhoon Warning Centre noted it as a 'Tropical Storm' and designated it as BOB 01B (JTWC). The present report deals with the effects of the cyclone Remal on the estuarine ecosystem of the Hooghly river and the surrounding Sundarban area with the aim of establishing relationships among the large array of selected physico-chemical and biological variables (with emphasis on the biooptical constituents) as well as to focus on the resiliency of the ecosystem itself to such natural catastrophes by comparing data recorded before and within a month of the incident from the selected study sites, based on the governing hypothesis that a well mixed estuary might withstand the effects of cyclones without triggering long term changes in it.

II. MATERIAL AND METHODS

Study Area

The study site is located at the Indian Sundarban at 21°32' - 21°60' N and 88°05' - 89° E. This natural mangrove forest is a part of the estuarine system of the river Hooghly (Ganges) NE coast of Bay of Bengal. It is the largest delta on the globe (world heritage site, http://www.unesco.org/en/list452), and a unique bioclimatic zone for its biodiversity of mangrove flora and fauna both in the land and water. The main artery of this ecosystem, the river Ganges along with its several distributaries, meets in Bay of Bengal forming India's largest estuarine complex. Lower part of this estuarine system is crisscrossed by numerous creeks and wide distributaries and several marshy islands are formed. Nine sampling stations (Fig. 1) have been selected viz. Harinbari (21.7440°N, 88.0616°E), Beguakhali (21.6573°N, 88.0387°E), Gangasagar (21.6276°N, 88.0739°E), Chemaguri (21.6770°N, 88.1604°E), Frasergunj (21.5738°N, 88.2302°E), Bakkhali (21.5507°N, 88.2585°E), Henry Island (21.5689°N, 88.3075°E), Lothian Island (21.7069°N, 88.3144°E), and G plot (21.6948°N, 88.4221°E) along the stretch of the Hooghly-Matla estuarine complex.

Sample Collection and variables studied

The sampling year was divided into three chief seasons, viz. Premonsoon (March-June), Monsoon (July-October), and Post Monsoon (November-February). The sampling frequency was monthly for the period of premonsoon of 2023 to post monsoon of 2024, followed by bimonthly during the premonsoon'2024-post monsoon"2025 period. The surface to near surface water samples were collected in using Niskin water sampler from each of the preordained stations. The actual depth of the collection was determined by the Secchi disc. The chosen ecological variables for the study were – Air Temperature or aT (ºC); Water Temperature or wT (ºC); pH; Salinity or Sal (psu); TSM or total suspended material ($mg.L^{-1}$); Dissolved Oxygen or D.O. ($mg.L^{-1}$); Primary Productivity or G.P.P ($mgC.m^{-3}.hr^{-1}$); dissolved micronutrients such as Nitrite-Nitrogen or NO_2-N (µM), Nitrate-Nitrogen or NO_3-N (µM), Ammonia/Ammonium-Nitrogen or (NH_3+NH_4)-N (µM), and Total Nitrogen or TN (µM); dissolved Phosphate-Phosphorus or PO_4-P (µM) and Total Phosphate or TP (µM); dissolved Silicate-Silicon or SiO_4-Si (µM); Chlorophyll *a* or Chl *a* ($mg.m^{-3}$); CDOM as absorption coefficient (m^{-1}); Phytoplankton Density or Phyto.Den ($Cells.L^{-1}$) etc.

Measurements and Analyses

The near surface aT and surface to near surface wT were measured at each station using an on-board weather station. Wind velocity was measured using handheld anemometer. The mean of three Secchi disc depths was considered as the transparency of water at each station (Preisendorfer, 1986; Lee et al., 2015). TSM was measured as the dry weight difference between a pre-oven dried and weighted inert filter prior to filtration and following filtration, of uniform volume of water, containing the residues. The water samples were stored in triplicates in acid cleaned TARSONS™ inert HDP narrow mouth containers of 1 L capacities; phytoplankton samples were collected, using 20 µM bolting silk nets, in wide mouth containers and were preserved using a combination of 2% (v/v) buffered formalin and 2.5% (v/v) acidic Lugol's iodine solution (Mukherjee et al., 2014). No chemical preservatives were used for the water

samples intended to be used in physico-chemical and hydrological variable analyses.

The water samples were transferred to ice boxes immediately following collection and brought to the laboratory on the very same day. Salinity and pH were both measured after returning to the laboratory as well with the aid of a bench top pH meter [model-HI2222] by Hanna^R instruments and argentometric titration following the Mohr-Knudsen method (Grasshoff et al., 1983, 1999) respectively. Meteorological data were procured from local relevant agency.

The water samples upon reaching the laboratory were brought to room temperature by placing them inside an incubator set at 25ºC. Once acclimatized, the samples were subjected to vacuum filtration through 0.7 µm GF/F inert filters. All the analyses involving the dissolved variables were performed with the filtered samples.

The sampling of CDOM was performed following Nelson and Siegel (2002), Mannino et al. (2008), and Dall'Olmo et al. (2012). Water samples for CDOM were subjected to filtration through 0.7 µm GF/F inert filter paper followed by another filtration through 0.2 µm Nucleopore membrane filter. The filtrates were stored immediately in amber colored borosilicate glass bottles and placed within a cold box for transportation. These were transported back to the laboratory as soon as possible. Prior to analysis using a Shimadzu^R spectrometer, the samples were brought to room temperature to avoid the temperature difference between samples and the blank. As stated in a similar study by De et al. (2020), CDOM estimations involved the understanding that the calculated results were directly proportional to the sample optical density relative to the pure water reference after correction for the pure water blank and specification of a null absorption. The absorption was measured within 350-750 nm, especially at 380, 412, 443, 490 and 547 nm respectively, after the equation $\mathbf{A(\lambda) = 2.303*[(OD_s(\lambda) - OD_{bs}(\lambda)) - OD_{null}]/L}$, where 2.303 is the conversion factor in converting a natural log to a base-10 log); '**A(λ)**' is the absorption coefficient at specific wavelength, 'L' is the distance between the walls of the cuvette or the light travel path length, 'OD_s (λ)' is the optical density of the filtrate sample relative to extensively purified water at specific wavelength, 'OD_{bs} (λ)' is optical density of a purified water blank treated like a sample relative to purified water, and OD_{null} is the apparent residual optical density at a long visible or near infrared wavelength where absorption (attenuation) by dissolved materials is assumed to be zero (Bricaud et al. 1981; Stedmon et al. 2000).

Dissolved Oxygen was measured using a very high precision portable D.O. meter [model-HI2004] by Hanna^R instruments as well as using the chemical analytic method using Manganese Sulphate and Potassium Iodide (Strickland and Parsons, 1972). The primary productivity (gross and net) and respiration (community) were calculated using the light and dark bottle method (Strickland and Parsons, 1972). The bottle incubated for primary productivity rate measurements were filled with water filtered through a piece of 60µm mesh sized zooplankton net to minimize the grazing and oxygen consumption.

All the dissolved micronutrients treated as variables of the study were estimated/measured following protocols laid down by Grasshoff et al. (1983, 1999) and APHA (1998).

Dissolved inorganic nitrogen species such as NO_2-N and NO_3-N were estimated spectrophotometrically after diazotization using n-Ethylene Diamine Dihydrochloride and Sulphanilamide. In case of the latter, it was first reduced by passing the filtered water samples through a Copperised-Cadmium (Cd^{2+}- Cu^{2+}) column where NO_3-N was converted to NO_2-N. Reduced nitrogen as (NH_3+NH_4)-N was estimated spectrophotometrically using the Phenol-Hypochlorite reaction method (Phenol-Indophenol complex) in the presence of a Citrate buffer.

To estimate the concentration of TN and TP, the respective samples were first autoclaved in presence of an oxidizing agent such as Persulphate. This method simultaneously converts ammonia and inorganic nitrogen (except dinitrogen) to nitrates and organic forms of phosphorus to orthophosphates. Dissolved PO_4-P was estimated spectrophotometrically following the formation of Molybdenum Blue complex.

Dissolved SiO_4-Si was determined in the water samples using Ammonium Molybdate to form Molybdosilicic complex which was then measured using a Vis-UV spectrophotometer.

In order to obtain Chl *a* data from each of the preselected stations, centrifuge tubes containing 95% analytical grade acetone were used and filtered residues from each station were placed respectively; following a steeping period of 24 hours at 0-4ºC the tubes were sonicated (five pulses of 90 Hz at intervals of 30 seconds) and then centrifuged at 10000 rpm for 10 minutes. The verdant supernatant was used for spectrophotometrically estimating the Chl *a* content (Hiscox and Israelstam, 1979; Strickland and Parsons, 1972; Yentsch and Menzel, 1963). Especially for the chlorophyll estimation, the filter paper and the residues were

treated with aliquot of Magnesium Carbonate to prevent degradation of chlorophyll into phaeophytin.

The Ocean Color Monitor 3 satellite data was used to procure Chlorophyll *a* and TSM values for the relevant months pertaining to the selected stations were procured from SENTINEL 3 of European Space Agency (https://sentinels.copernicus.eu/web/sentinel/copernicus/sentinel-3) and BHOONIDHI of National Remote Sensing Centre, India (https://bhoonidhi.nrsc.gov.in/bhoonidhi/index.html) and the resolution set for the openly accessible data was in the range of 100m-1Km. The OCM and *in situ* data have been corroborated wherever applicable through correlation, at 0.05 level of significance.

III. RESULTS

A plethora of environmental variables of meteorological, physico-chemical, and biological in nature (as well as derivatives) have been considered for the present study to serve as guiding parameters which are.

The procured spatio-temporal (Fig. 2) data on Rh showed the values to be relatively higher at the stations near the confluence of river and sea, in addition to those in association with dense mangrove forests. The values were generally high in the Pre-Remal month compared to the Post Remal month, with the overall mean value to be 79.73%. Although it needs to be mentioned that station wise the data had not always indicated the same with few stations registering relatively higher values in post Remal period also, the discernible pattern is only observable when the study site was considered entirely.

A similar trend was observed in case of precipitation (Fig. 3) where sites nearer to larger expanse of water had incidentally registered higher values. Again, August was comparatively wetter than the rest of the months. The highest value was recorded in Ganga Sagar, at 200.00 mm and at a mean 163.32 mm in the Pre-Remal month. It also had registered far greater average precipitations at 68.82 nm, compared to 19.63 mm of Post Remal month.

Wind velocity (Fig. 4) data was understandably found to be quite coherent with the earlier two variables observed where sites more expansive and physically unhindered had shown higher values in general, with those recorded during Post Remal being relatively higher. On average the recorded wind velocity across all the selected sites was 6.27 ms^{-1}, evidently higher than the mean 5.63 ms^{-1} observed in the Pre-Remal month.

The values of aT (Fig. 5) observed during the sampling episode had as much to do with the spatiotemporal characteristics of the sites as with the time of sampling, with sites traversed during the latter part of the day registering higher temperatures than the ones completed earlier in the day. Pre-Remal month had registered lower values in general at around 32°C, in comparison to the Post Remal month where an average of over 35°C was observed across the sites; the highest among them was recorded in Frasergunj at 39.26°C.
The wT values were also governed significantly by the air temperature, where wind velocity had also played a considerable part as well. Comparatively higher values of water temperature (Fig. 6) were recorded during the Post Remal, with an across-the-sites mean value of 32.53°C to that of 30.01°C, the mean observed during Pre-Remal period. Here too, data from Frasergunj had shown to be comparatively higher at 33.30°C among the preselected study sites during Post Remal survey.

The pH (Fig. 7) value depends on several factors, among the more important of which some of the more important ones are the extent of seawater and freshwater mixing, sediment resuspension, and volume of discharge. An overall higher comparative value was observed in the Pre-Remal month at a mean of 7.92. The Post Remal mean was observed at 7.68.

The patterns of variations in salinity (Fig. 8) in the waters of the sampling sites were akin to pH as the latter is largely governed by former. The stations nearer to the Bay of Bengal had thrown up relatively higher values. The maximum salinity however was recorded from Bakkhali (24.57 psu) in Post Remal, although the mean salinity was comparatively low along the sites during that period. The Pre-Remal period had registered higher mean at 22.48 psu.

The months with higher precipitation (Fig. 9) incidentally also had registered the greater TSM. The Post Remal period, fresh from the effects of Remal had registered an altogether higher mean (46.84 mgL^{-1}) than Pre-Remal (26.85 mgL^{-1}). The most turbid water was observed at Beguakhali (61.79 mgL^{-1}) during the Post Remal month, followed closely by Harinbari, incidentally which was the highest (43.56 mgL^{-1}) during in the Pre-Remal month.

The D.O. (Fig. 10) values recorded in the Post Remal month were generally marginally higher in all the sampling sites (5.53 mgL^{-1}, in comparison to 5.26 mgL^{-1} observed in Pre-Remal month), with Henry Island showing a value of 6.07 mgL^{-1}; closely followed by other coastal/seaward sites. The D.O. values during Pre-Remal and Post Remal periods had ranged between 4.45 – 6.07 mgL^{-1}.

The highest dissolved NO_3-N (Fig. 11) value of 28.91 µM was recorded from Chemaguri with Henry Island, Frasergunj, and Bakkhali on heels during the Post Remal month. With a yielded mean value of 21.92 µM, it was documented to be quite high relative to the data obtained during Pre-Remal period (12.20 µM) and all the sampling stations had unanimously registered higher nitrate values compared to Pre-Remal months.

Pre-Remal period had revealed higher mean dissolved NO_2-N (Fig. 12) values than Post Remal months across the sampling sites (0.62 µM in case of the former; 0.32 µM corresponding to the latter). The highest value of 0.96 µM was recorded from Gangasagar during Pre-Remal period while the lowest value was exhibited in G-plot, at 0.13 µM, in the Post Remal month.

Similar to the pattern observed with nitrite, Pre-Remal month had revealed higher mean dissolved (NH_3+NH_4) - N (Fig. 13) as well, in comparison to Post Remal month (with the latter registering 3.69 µM and the former, 4.64 µM). The highest value of 6.62 µM was recorded from Bakkhali in Pre-Remal month. Incidentally, the same sampling site had yielded the highest ammonia value in Post Remal month also.

Total nitrogen (TN) data (Fig. 14) had been observed to corroborate the patterns observed in case of dissolved NO_3-N more closely than the rest of the nitrogen species relevant to the study concerned. The highest value of 197.92 µM was recorded from Beguakhali with the rest of the sites not far behind during Post Remal month. The Pre-Remal had registered a mean overall value of 92.28 µM in contrast to the 167.12 µM recorded during Post Remal month.

The dissolved PO_4-P(Fig. 15) values had revealed Post Remal month documenting higher mean values than what was observed prior to the onset of cyclone Remal (2.83 µM in case of Post Remal to 1.54 µM of Pre-Remal). The highest value of 3.51µM was recorded from Bakkhali during Post Remal month sampling and the lowest was recorded from Lothian Island in Pre-Remal phase (1.20 µM).

Total phosphorus (TP) (Fig. 16) had reflected a different pattern than what was observed with dissolved PO_4-P. In general, the Pre-Remal month showed a higher mean trend (9.76 µM) compared to Post Remal (7.39 µM) across the sampling sites. The highest value of 10.67 µM was recorded from Frasergunj, with Beguakhali being very similar (10.33 µM); whereas the lowest values among the two phases of sampling was observed in Harinbari, registering a value of 5.23 µM in Pre-Remal month.

Far greater mean dissolved SiO_4-Si (Fig. 17) was recorded during Pre-Remal (71.28 µM) than in Post Remal period (47.73 µM). At 85.18 µM, Chemaguri was the station with highest dissolved SiO_4-Si during the period of the study, while Gangasagar with 55.88 µM was the highest value observed during the Post Remal month, with other seaward facing sites registering more or less similar values throughout. The tentative range of recorded SiO_4-Si was 38-85 µM across the stations, taking into account both the cyclone demarcated sampling episodes.

Comparatively much higher values of Chl *a* (Fig. 18) were recorded during Post Remal with mean value at 5.78 $mg.m^{-3}$, compared to a mean of 4.75 $mg.m^{-3}$ observed during Pre-Remal phase of the study across all the sampling sites. Bakkhali had registered the highest values at 7.32 $mg.m^{-3}$ with the stations of similar environmental signatures among the selected ones not lagging far, therefore, underlining a general proliferation of chloroplast bearing organisms. In Pre-Remal, at Harinbari the lowest Chl *a* value was recorded (mean 3.26 $mg.m^{-3}$).

Post Remal month had yielded relatively higher mean PP values (55.87 $mgCm^{-3}hr^{-1}$) compared to the mean Pre-Remal value (40.51 $mgCm^{-3}hr^{-1}$) (Fig. 19) observed across all the concerned sampling stations. The coastal sites and the ones with mangrove association viz. Gangasagar, Bakkhali, Frasergunj, Lothian Is. and G plot had all registered values higher than 40 $mgCm^{-3}hr^{-1}$ with waters near Lothian island yielding the highest value of 72.92 $mgCm^{-3}hr^{-1}$, followed closely by Frasergunj (67.71 $mgCm^{-3}hr^{-1}$).

The densest population assemblages of phytoplankton (Fig. 20) sampled by 20-micron net was observed at Lothian island with value 4.32×10^5 $CellsL^{-1}$ and Frasergunj being nearly similar in range of the observed data during Pre-Remal month (mean value across stations: 2.60×10^5 $CellsL^{-1}$, compared to 1.23×10^5 $CellsL^{-1}$ in Post Remal month). All the stations had registered phytoplankton density values at more than 1.50×10^5 $CellsL^{-1}$ uniformly along the studied sites during Pre-Remal month, a fact that cannot be stated for those stations following the event of Cyclone Remal.

Normalized CDOM had shown (Fig. 21) the highest absorbance at 350-380nm (the UV B-C region), followed by maxima in 443 nm and 532 nm respectively, almost uniformly during Pre-Remal, across all the selected study sites. However, Post Remal month had demonstrated a stark difference to that as the absorption maxima were no longer grouped uniformly and apart from the UV region of the selected spectral range,

412 nm, 443 nm, 532 nm, and 547 nm etc. had all reported their respective maxima based on the samples recovered from various stations, especially an decrease in sites dominated by marine waters. The disruption in the CDOM grouping could be clearly attributed to the massive ecological perturbance brought about by 'Remal'. The actual overall mean absorbance or A_{CDOM} had ranged between 4.627 m^{-1} and 5.387 m^{-1} during Pre-Remal period, in comparison to the range of 4.617 m^{-1} to 4.828 m^{-1} in Post Remal month.

IV. DISCUSSION

Cyclones, whether of moderate intensities or really large, often tend to disrupt the normal tidal prism of a well mixed tropical estuary, either by ephemeral manipulation in the dissolved nutrient load and salt concentrations in addition to the associated physico-chemical variables, or by introducing newer materials to a section of the river that otherwise never encounters such compounds in general. As the storms bring in rain inland, they wash away all sorts of soil and dirt, and drastically alter the quantity of the introduced organic matter that gets flushed from the inland watershed into the estuary. Cyclone 'Remal' was a tropical storm that did the same as was observed from the results obtained from the water quality monitoring and analyses (Figs. 2 – 21; Tables 1-2) to the Hooghly-Matla estuarine ecoregion on northwest Bay of Bengal.

Analytical outcomes on physiochemical variables in pre- and post storm months from the selected sampling points showed no stark difference ($P>0.1$) in chemical profiles due to seasonal variability, underlining that the geochemical parameters of could revert to pre-storm scenario in a given span of time, which for the ecoregion concerned might have taken less than two months, based on the near consistent data observed after a month since the episode of 'Remal'. This is quite consistent with the previous studies performed on other similar estuarine settings (Paerl and Paul, 2012; Zhang et al., 2014) of the lower Pearl River.

Cyclone Remal's impact could be summarized into three a three-pronged effect of large scale intrusion of seawater into the river owing to the storm surge, riverine flood induced by Remal induced rainfall, and rise in water level due to the synchrony with the astronomical tide of the Bay of Bengal itself. All these had ensured changes in the ambient salinity, whether by enrichment or dilution, depending on the specific section of the Hooghly-Matla river complex. A very similar event had taken place in the Mississippi River estuary and Bay of St. Louis estuary following Hurricane Gustave and Ike, as was documented in the works of Wang et al. (2010) and Bonvillain et al. (2011) respectively.

Lower Relative humidity, precipitation, pH, and salinity after a month from the onset of Cyclone Remal in spite of registering higher TSM and D.O. (Figs. 2-10) in comparison to a month prior at the selected sampling sites might appear to be contradictory to the conventional wisdom of estuarine study, but given the well-mixed positive, micro-mesotidal nature of the estuary (Mukhopadhyay et al., 2006; Nandy and Bandyopadhyay, 2011) and the gradual addition of the flood water from inland watersheds into the estuary sink, a phenomenon observed throughout the world in tropical estuaries following an event of cyclones/hurricanes (Devi et al., 2021; Medeiros, 2022), the observed responses appear to be quite consistent with the earlier studies on the same ecoregion following such atmospheric turbulent conditions (Mukherjee et al., 2012; Mukherjee et al., 2013; Paul et al., 2020; Devi et al., 2021).

Although cyclone brings in large scale salinity changes, more or often increasing it, an effect which Bay of Bengal is not impervious to (Xu et al., 2020; Chaco and Jayaram, 2022), the presently reported study had revealed rather lower recorded surface water salinity values following the Cyclone Remal which could be attributed to the well documented phenomena of advection of superficial freshwater from cyclone induced precipitations.

The higher concentrations of dissolved inorganic plant nutrients (Figs. 11-17) such as nitrates, total nitrogen, phosphates, total phosphates, and silicates following the cyclone was expected as large scale sediment resuspension of mangrove sediments and land wash in the form of riverine run off was introduced from surrounding agricultural lands and upriver. In addition to these, greater offshore mixing in the wake of a tropical storm such as cyclones also contribute to greater introduction of such nutrients in the surface water as had been previously documented by (Shiah et al., 2000; Mukherjee et al., 2013). Tropical storms can enhance nutrient cycling and buildup in deep waters, raising the danger of eutrophication and cyanobacterial dominance in estuaries (Stockwell et al., 2020). The steep and prolonged increases in total nitrogen, ammonium nitrogen, and total phosphorus in the deep offshore waters and over-the-shelf coastal waters following cyclones may increase the risk of eutrophication and cyanobacterial dominance when these nutrients eventually reach the surface waters due to mixing disturbances. Cyclone-driven greater ammonium-nitrogen release rates, together with oxygen depletion owing to mineralization, may accelerate phosphorus release by boosting alkaline phosphatase activity (Ma et al., 2018). While not exactly supporting the observations of the presently reported study but, similar reports effects on nutrient availability and

cycling following tropical cyclones/storms in some recent studies by Bhattacharya et al. (2025), Chen et al. (2023), and Purnaningtyas et al. (2021) where disruptions or enhancements in nutrient loading were the outcomes which had reflected in the phytoplankton blooms or the delay in their planktonic assemblages thereof.

But strangely, the Hooghly estuary had shown lower nitrite- and ammonium-nitrogen values within a few weeks of the passage of cyclone Remal, indicating the oxygen enrichment through atmospheric mixing as well as increased primary chlorophyll *a* contents and productivity (Figs. 18 and 19), in spite of considerable reshuffling of the phytoplankton composition since the consistent nature of the phytoplankton densities observed in pre-Remal months had been visibly affected by the cyclone itself, with post-Remal compositions revealing many stenohaline species as well across the selected sites (Fig. 20). Recently, Shi et al. (2025), Thompson et al. (2022), Wang et al (2021) etc. have published their observations on long term effects of cyclonic storms, whether sporadic or sequential, on coastal phytoplanktonic assemblages where some of the features, such as nutrient loading and reverting to the pre cyclonic state in case of phytoplankton community composition, have corroborated with some of the observed features of the current study, although the relatively faster rate of achieving pre-cyclonic conditions in Hooghly estuary remains a uniqueness of it.

In coastal areas, it has been observed that the community composition of phytoplankton can be influenced by tropical cyclones (TCs), leading to rise in dinoflagellates and occasionally diatoms (Tsuchiya et al., 2014; Anglès et al., 2015; Paerl et al., 2018). The specific way in which phytoplankton reacts is said to depend on the characteristics and timing of the storm. Limited data from a few locations in the northern hemisphere suggest that wet storms with higher levels of runoff may favour the growth of dinoflagellates, particularly in the latter half of the year. In some instances, the swift changes in phytoplankton species over a matter of days indicate that significant effects in coastal regions can be attributed to advection (Peierls et al., 2012; Hall et al., 2013; Harding Jr. et al., 2016).

The observed phytoplankton composition from Hooghly estuary following the cyclone Remal have also pointed towards the same trend of dinoflagellate and diatom enrichment, that too within a period of couple of weeks since the passage of the cyclone where the decrease in overall density simply been countered by the increase in species richness (Shannon-Weiner's diversity index had shown an increase from 1.92 to 2.65 following Cyclone Remal) owing to the temporary shift from the usual stoichiometry of the water column. Table 1 highlights this fact even more as mean overall increase in Chl *a* contents, obtained from Oceansat 3 (the phytoplankton cells thereby affecting TSM) and apparent increase in stenohaline species (Table 2) in post-Remal waters even after about a month (~20 days) across all the selected study sites fully corroborate with the other *in situ* recorded variables. The absorption coefficient of CDOM changes either over time as downwelling irradiance causes photodegradation or photo-oxidation of the material in the upper layer of the ocean, or with depth because CDOM molecules experience reduced irradiance at greater depths, resulting in lower rates of photodegradation (Vodacek et al., 1997; Chen and Bada, 1992; Siegel and Michaels, 1996). In a well-mixed estuary, the vertical variation in CDOM absorption coefficient is less significant compared to that in a stratified estuary, where a strong thermocline creates a barrier that separates water masses above, which are exposed to higher irradiance and therefore undergo more photodegradation.

In a study by Hoge and Lyon (2002), it has been put forth that absorption of CDOM returns to levels seen before the hurricane within approximately 10 to 15 days in water further offshore in stratified estuaries, while takes longer in well-mixed ones. The increase in the CDOM absorption coefficient remains for a somewhat extended duration at about 75–150 km to the right of the storm's path. While there is an observable change in the CDOM absorption coefficient in the aftermath on both sides of the storm's track, the increase is more pronounced on the right side compared to the left which in some cased have somewhat lowered following a storm.

This symmetry on the left and asymmetry on the right regarding the CDOM absorption coefficient aligns with earlier researches based on satellite observations (Stramma et al., 1986; Shay et al., 1992), data from drifting buoys (Black et al., 1988), and measurements from CTD and acoustic current profilers (Church et al., 1989), among others. From Fig. 21 it can be observed that the stations lying on the cyclone track, or on its left (the stations were either within the cyclone track or on its left-side) have all shown decreased CDOM absorption coefficients attributable to increased marine influence on account of the cyclone. It is also notable that due to the well mixed nature of the estuary, the freshwater influence after a few weeks (~20 days of the passage of the storm) has begun to take over as the values had started to approach the pre-Remal readings. All these are in vindication to the earlier recorded data on similar estuarine environments following tropical storms.

V. CONCLUSION

The Hooghly estuary, being vertically well-mixed and meso-microtidal in nature was found to withstand the

effects of the severe cyclone 'Remal' by preventing any long-term changes in the ecosystem from taking hold as pre-storm situations were observed only after a few weeks of the passage of the storm which had made landfall through the estuary itself. In this context, the damage, or rather the changes brought about by it to the ecosystem should have been much pronounced, as it was anticipated, than what was actually observed. The change in salinity or pH due to the immensely increased load of land wash and marine tide surge that would have made any other stratified estuary far removed from its general stoichiometric setting, had only been observed to merely modify the environment to an extent. Shifts in general phytoplankton population, owing to an increased nutrient load, was only confined to introductions of more stenohaline species along with the already existing euryhaline ones without affecting the overall density of the population had underlined the resiliency of the ecosystem against any drastic changes. The governing hypothesis of resistance of a well mixed estuary against disruptive effects of a tropical storm was, albeit not conclusive, satisfactorily tested in case of Hooghly-Matla estuarine complex. Further such studies are intended to fully understand the role of such ecosystems in maintain environmental stability following meteorological mayhems as estuaries are among the most productive ecosystems, both ecologically and economically, in the world.

VI. ACKNOWLEDGMENT

The financial aid sponsored by the Space Applications Centre of ISRO, India for this collaborative study with the University of Calcutta is highly appreciated. We extend our thanks to the Department of Forestry, and Directorate of Sundarban Biosphere Reserve, Govt. of West Bengal for providing us with the crucial logistical support to carry out the studies across the selected sites.

CONFLICT OF INTEREST

The authors do hereby claim that there exist no conflicts of interests among them or with anyone else regarding the execution of the work, publication of data, as well as the roster hierarchy.

REFERENCES

[1] American Public Health Association (APHA). "Standard methods for the examination of water and wastewater," 20th Edition, Jointly published by American Public Health Association, American Water Works Association and Water Environment Federation, 1998.

[2] Anglès, S., A. Jordi and L. Campbell, "Responses of the coastal phytoplankton community to tropical cyclones revealed by high-frequency imaging flow cytometry," in Limnol. Oceanogr., vol. 60, pp. 1562–1576, 2015.

[3] Bhattacharya, T., P. K. Ghosal and K. Chakraborty, "Biogeochemical Response to Tropical Cyclones in the Northern Indian Ocean: Understanding and Gray Areas," in JGR Oceans, vol. 130, no.8, e2025JC022540, 2025.

[4] Biswas, A.N., "Geohydro-morphometry of Hooghly estuary," in J. inst. Eng. (India), vol. 66, pp. 6-73, 1985.

[5] Black, P. G., R. L. Elsberry, L. K. Shay and J. D. Hawkins, "Atmospheric boundary layer and oceanic mixed layer observations in hurricane Josephine obtained from air-deployed drifting buoys and research aircraft," in J. Atmos. and Oceanic Tech., vol. 5, pp. 683–698, 1988.

[6] Bonvillain, C.P., B. T. Halloran, K.M. Boswell, W. E. Kelso, A.R. Harlan and D. A. Rutherford, "Acute physiochemical effects in a large river-floodplain system associated with the passage of Hurricane Gustav," in Wetlands, vol. 31, 979e987, 2011.

[7] Bricaud, A., A. Morel and L. Prieur, "Absorption by dissolved organic matter of the sea (yellow substance) in the UV and visible domains," in Limnol. Oceanogr., vol. 26, pp. 43–53, 1981.

[8] Chaco, N. and C. Jayaram, "Response of the Bay of Bengal to super cyclone Amphan examined using synergistic satellite and in-situ observations," in Oceanologia, vol. 64, no. 1, pp. 131-144, 2022.

[9] Chen,F., Q. Lao, X. Lu, C. Wang, C. Chen, S. Liuand X. Zhou, "A review of the marine biogeochemical response to typhoons," in Mar. Pollut. Bull., vol. 194, no. B, pp. 115408, 2023.

[10] Chen, R. F. and J. L. Bada, "The fluorescence of dissolved organic matter in seawater," in Marine Chemistry, vol. 37, pp. 191–221, 1992.

[11] Church, J. A., T. M. Joyce and J. F. Price, "Current and density observations across the wake of hurricane Gay," in J. Phys. Oceanogr, vol. 19, pp. 259–265, 1989.

[12] Dall'Olmo, G., E. Boss, M. Behrenfeld, T. Westberry, "Particulate optical scattering coefficients along an Atlantic meridional transect," in Opt Express, vol. 20, no. 19, pp. 21532–21551, 2012.

[13] De, T. K., M. Raman, S. K. Sarkar and A. Mukherjee, "Ecological assessment of Hooghly River considering a few of the more perturbed sites based on some relevant physicochemical and biological variables – A part of the AVIRIS-NG (NASA-ISRO) ground truth verification," in Reg. Stud. Mar. Sci., vol. 41, 101598, 2021.

[14] Devi, M., S. Patgiri, A. Medhi, S. Das, A.K. Barbara and M. Saikia, "Impact of amphan cyclone on environment modification," in Geomatics, Natural Hazards and Risk, vol. 12, no. 1, pp. 3114-3139, 2021.

[15] Grasshoff, K., K. Kremling and M. Ehrhardt, "Methods of seawater analysis," 2nd Ed., Wiley-VCH, Weinheim, New York, 1983.

[16] Grasshoff, K., K. Kremling and M. Ehrhardt, "Methods of seawater analysis," 3rd Ed., Wiley-VCH, Weinheim, Germany, 1999.

[17] Hall, N.S., H.W. Paerl, B.L. Peierls, A.C. Whipple and K.L. Rossignol, "Effects of climatic variability on phytoplankton biomass and community structure in the eutrophic, microtidal, New River Estuary, North Carolina, USA," in Est. Coast. Shelf Sci., vol. 117, pp. 70–82, 2013.

[18] Harding, L. W. Jr., M. M. Mallonee, E. S. Perry, W. D. Miller, J. E. Adolf, C. L. Gallegos and H. W. Paerl, "Variable climatic conditions dominate recent phytoplankton dynamics in Chesapeake Bay," in Sci. Rep., vol. 6, 23773, 2016.

[19] Hiscox, J.D. and G.F. Israelstam, "A method for the extraction of chlorophyll from leaf tissue without maceration," in Can. J. Bot., vol. 57, pp. 1332-1334, 1979.

[20] Hoge, F. E. and P. E. Lyon, "Satellite observation of chromophoric dissolved organic matter (CDOM) variability in the wake of hurricanes and typhoons," in Geophysical Research Letters, vol. 29, no. 19, 1908, 2002.

[21] IMD: "Tropical Weather Outlook for North Indian Ocean". Indian Meteorological Department. Archived from the original on 25 May 2024. Retrieved 25 May 2024.

[22] JTWC: Tropical Cyclone 01B (One) Warning No. 1 (Report). United States Joint Typhoon Warning Center. 25 May 2024. Archived from the original on 25 May 2024. Retrieved 25 May 2024.

[23] Lee, Z., S. Shang, C. Hu, K. Du, A. Weidemann, W. Hou, J. Lin and G. Lin, "Secchi disk depth: A new theory and mechanistic model for underwater visibility," in Remote Sens. Environ., vol. 169, pp. 139–149, 2015.

[24] Ma, S.N., H.J. Wang, H.Z. Wang, Y. Li, M. Liu et al., "High ammonium loading can increase alkaline phosphatase activity and promote sediment phosphorus release: a two-month mesocosm experiment," in Water Res., vol. 145, pp. 388–397, 2018.

[25] Mannino, A., M.E. Russ and S.B. Hooker, "Algorithm development and validation for satellite-derived distributions of DOC and CDOM in the U.S. Middle Atlantic Bight," in J. Geophys. Res., vol. 113, no. C7, C07051, 2008.

[26] McDiffett, W.F., A.W. Beidler, T.F. Dominick and K.D. McCrea, "Nutrient concentration-stream discharge relationships during storm events in a first-order stream," in Hydrobiologia, vol. 178, no. 2, pp. 97-102,1989.

[27] Medeiros P.M., "The Effects of Hurricanes and Storms on the Composition of Dissolved Organic Matter in a Southeastern U.S. Estuary," in Front. Mar. Sci., vol. 9, 855720, 2022.

[28] Mukherjee, A., S. Das, T. Bhattacharya, M. De, T. K. Maiti, T. K. De, "Optimization of phytoplankton preservative concentrations to reduce damage during long-term storage," in Biopres. Biobank., vol. 12, no. 2, pp. 139-147, 2014.

[29] Mukherjee, A., S. Das, S., M. De, T. K. Maiti, "A Report on the Micro-Phytoplankton Size Range, Biovolume, Biomass and Geometric Shape in the Post "Aila" (Severe Cyclone) Waters of Estuarine Sundarban-Bay of Bengal, India," in J. Mar. Biol. Oceanogr., vol. 2, no. 4, pp. 11, 2013.

[30] Mukherjee, S., A. Chaudhuri, S. Sen and S. Homechaudhuri, "Effect of Cyclone Aila on estuarine fish assemblages in the Matla River of the Indian Sundarbans," in Journal of Tropical Ecology, vol. 28, pp. 405-415, 2012.

[31] Mukhopadhyay, S., H. Biswas, T.K. De and T.K. Jana, "Fluxes of nutrients from the tropical River Hooghly at the land-ocean boundary of Sundarbans, NE coast of Bay of Bengal, India," in J. Marine Syst., vol. 62, pp. 9-21, 2006.

[32] Nelson, N.B. and D. A. Siegel, "Chromophoric DOM in the open ocean," in Biogeochemistry of marine dissolved organic matter, Academic Press, San Diego, USA, pp. 547–578, 2002.

[33] Paerl, H.W., J.R. Crosswell, B. Van Dam, N.S. Hall, K.L. Rossignol, C.L., Osburn et al., "Two decades of tropical cyclone impacts on North Carolina's estuarine carbon, nutrient and phytoplankton dynamics: implications for biogeochemical cycling and water quality in a stormier world," in Biogeochemistry, vol. 141, pp. 307–332, 2018.

[34] Paerl, H.W. and V.J. Paul, "Climate change: links to global expansion of harmful Cyanobacteria," in Water Res., vol. 46, pp. 1349–1363, 2012.

[35] Paul, S., S. Karan and B.D. Bhattacharya, "Effects of cyclone Fani on the copepod community of the Ganges River estuary of India," in Environ. Monit. Assess., vol. 192, pp.763, 2020.

[36] Peierls, B.L., N.S. Hall and H.W. Paerl, "Non-monotonic responses of phytoplankton biomass accumulation to hydrologic variability: a comparison of two coastal plain North Carolina estuaries," in Estuar. Coasts, vol. 35, pp. 1376–1392, 2012.

[37] Preisendorfer, R.W., "Secchi disk science: Visual optics of natural waters," Limnol. Oceanogr., vol. 3, no. 5, pp. 909-926, 1986.

[38] Purnaningtyas, D. W., F Khadami and Avrionesti, "Nutrient enrichment induced by tropical cyclone Seroja

in the southeastern tropical Indian Ocean," in IOP Conf. Series: Earth and Environmental Science, vol. 925, 012021, 2021.

[39] Sadhuram, Y., V.V. Sarma, T.V.R. Murthy and B. Prabhakara Rao, "Seasonal variability of physico-chemical characteristics of the Haldia channel of Hooghly estuary, India," in J. Earth Syst. Sci., vol. 114, pp. 37-49, 2005.

[40] Shay, L.K., P.G. Black, A.J. Mariano, J.E. Hawkins and R.L. Elsberry, Upper ocean response to hurricane Gilbert," in J. Geophys. Res, vol. 97, pp. 20,227–20,248, 1992.

[41] Shi, H., Y. Chen, H. Zhou, R. Mortimer and G. Pan, "Impact of tropical cyclones on coastal phytoplankton blooms and underlying mechanisms." in J. Hydrol. Reg. Stud., vol. 59, 102389, 2025.

[42] Shiah, F.K., S.W. Chung, S.J. Kao, G.C. Gong and K.K. Liu, "Biological and hydrographical responses to tropical cyclones (typhoons) in the continental shelf of the Taiwan Strait," in Continental shelf research, vol. 20, no. 15, pp. 2029-2044, 2000.

[43] Siegel, D. A., and A. F. Michaels, "Quantification of non-algal light attenuation in the Sargasso Sea: Implications for biogeochemistry and remote sensing," in Deep-Sea Res., vol. 43, pp. 321–345, 1996.

[44] Stedmon, C.A., S. Markager and H. Kaas, "Optical properties and signatures of chromophoric dissolved organic matter (CDOM) in Danish coastal waters," in Estuar. Coast. Shelf. Sci., vol. 51, pp. 267–278, 2000.

[45] Stockwell, J.D., J.P. Doubek, R. Adrian et al., "Storm impacts on phytoplankton community dynamics in lakes," in Global Change Biol., vol. 26, pp. 2756–2784, 2020.

[46] Stramma, L., P. Cornillion and J. F. Price, "Satellite observations of sea surface-cooling by hurricanes," in J. Geophys. Res., vol. 91, pp. 5031–5035, 1986.

[47] Strickland, J.D.H. and T.R. Parsons, "A Practical Handbook of Seawater Analysis," 2nd Edition, Fisheries Research Board of Canada Bulletin, No. 167, Fisheries Research Board of Canada, pp. 310, 1972.

[48] Thompson, P.A., H.W. Paerl, L. Campbell, K. Yin and K.S. McDonald, "Tropical cyclones: what are their impacts on phytoplankton ecology?" in J. Plankt. Res., vol. 45, pp. 180-204, 2022.

[49] Tsuchiya, K., V. S. Kuwahara, T. Yoshiki, N. Ryota Hideo, K. Norikazu, T. Kikuchi and T. Toda, "Phytoplankton community response and succession in relation to typhoon passages in the coastal waters of Japan," in J. Plankton Res., vol. 36, pp. 424–438, 2014.

[50] A. Vodacek, N.V. Blough, M.D. De Grandpre, E.T. Peltzer and R.K. Nelson, "Seasonal variation of CDOM and DOC in the Middle Atlantic Bight: Terrestrial inputs and photooxidation," in Limnol. Oceanogr., vol. 42, pp. 674–686, 1997.

[51] Wang, T., S. Zhang, F. Chen et al., "Influence of sequential tropical cyclones on phytoplankton blooms in the northwestern South China Sea," in J. Ocean. Limnol., vol. 39, pp. 14–25, 2021.

[52] Wang, X., Y. Cai and L. Guo, "Preferential remove of dissolved carbohydrates during estuarine mixing in the Bay of St. Louis estuary in the northern Gulf of Mexico," in Marine Chemistry, vol. 119, 130e138, 2010.

[53] Xu, H., R. Yu, D. Tang, Y. Liu, S. Wang and D. Fu, "Effects of Tropical Cyclones on Sea Surface Salinity in the Bay of Bengal Based on SMAP and Argo Data," in Water, vol. 12, p. 2975, 2020.

[54] Yentsch, C.S. and D.W. Menzel, "A method for the determination of phytoplankton, chlorophyll, and phaeophytin by fluorescence," in Deep-Sea Res. Oceanogr. Abstr., vol. 10, pp. 221-231, 1963.

[55] Zhang, Y.S., S.H. Swinea, G. Roskar, S.N. Trackenberg et al., "Tropical cyclone impacts on sea grass-associated fishes in a temperate-subtropical estuary," in PLoS One, vol. 17, no. (10), e0273556, 2022.

[56] Zhang, S.W., L.L. Xie, Y.J. Hou, H. Zhao, Y.Q. Qi and X.F. Yi, "Tropical storm-induced turbulent mixing and chlorophyll a enhancement in the continental shelf southeast of Hainan Island," in J. Mar. Syst., vol. 129, pp. 405–414, 2014.

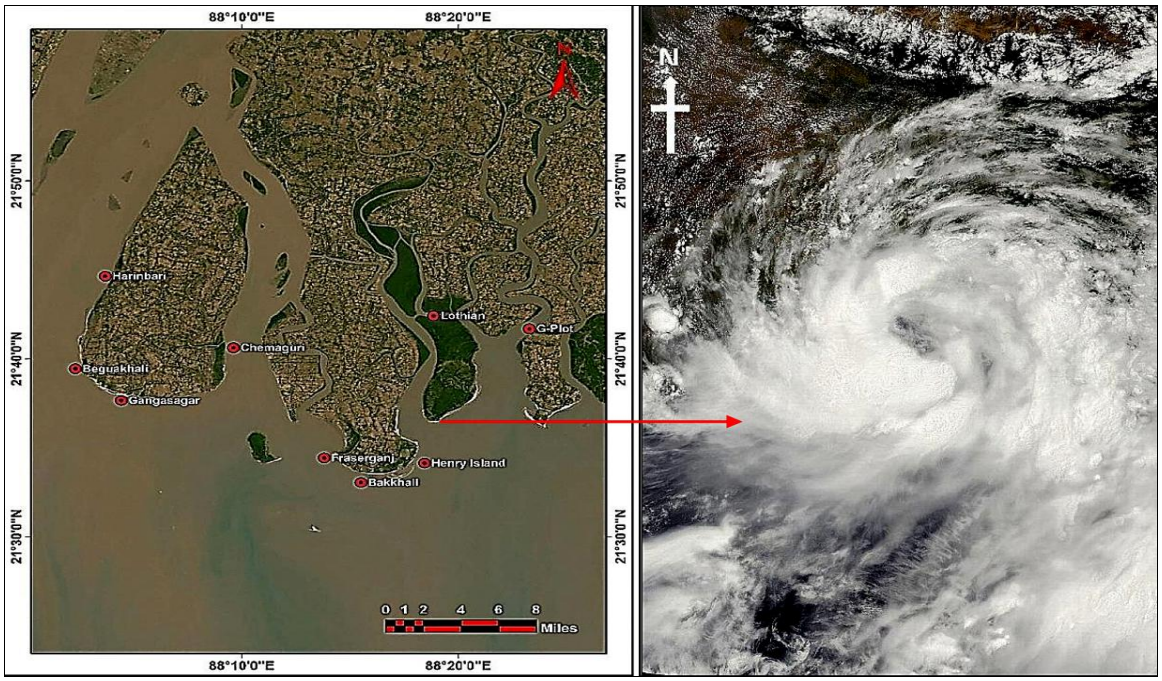

Fig. 1: Map of the study area denoting the selected sites of sampling and area of land fall of Sever Cyclonic Storm 'Remal' along the study area (https://en.wikipedia.org/wiki/File:Remal_2024-05-26_0740Z.jpg).

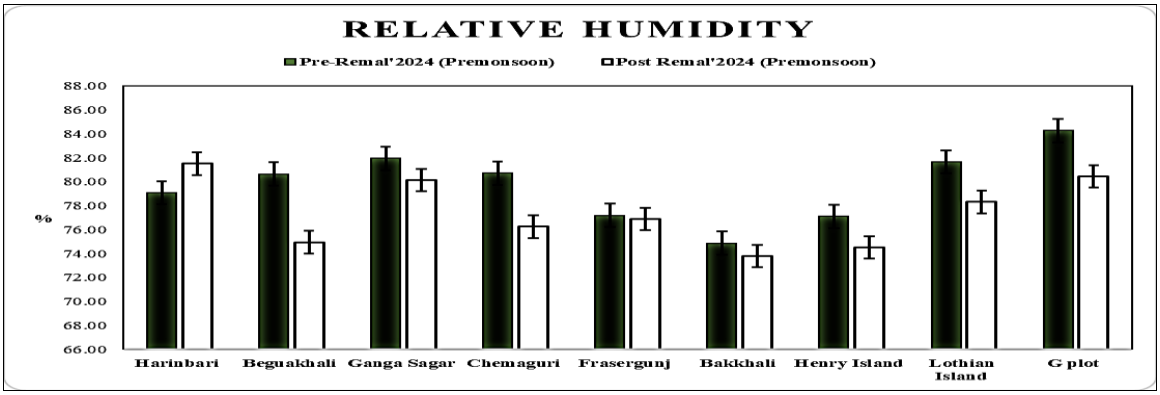

Fig. 2: Comparison in between the observed mean relative humidity recorded during the pre- and post 'Remal' sampling periods.

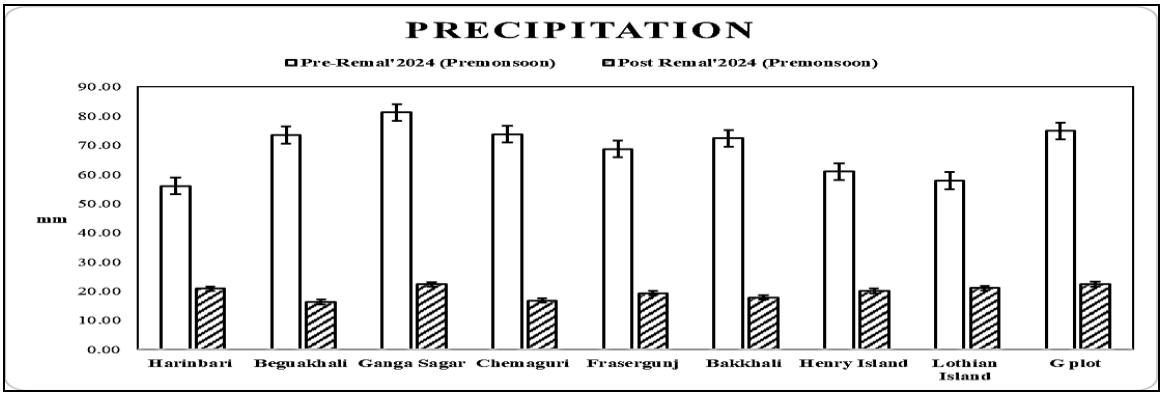

Fig. 3: The chart depicts the variation in precipitation at the selected sites before and after the occurrence of Cyclone Remal.

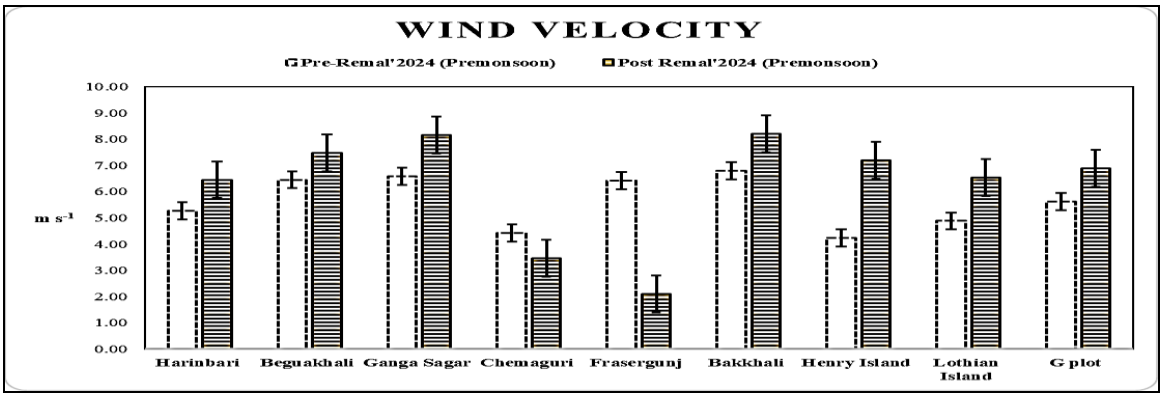

Fig. 4: The comparative account of wind velocity across the selected sampling sites, before and after the onset of Cyclone Remal

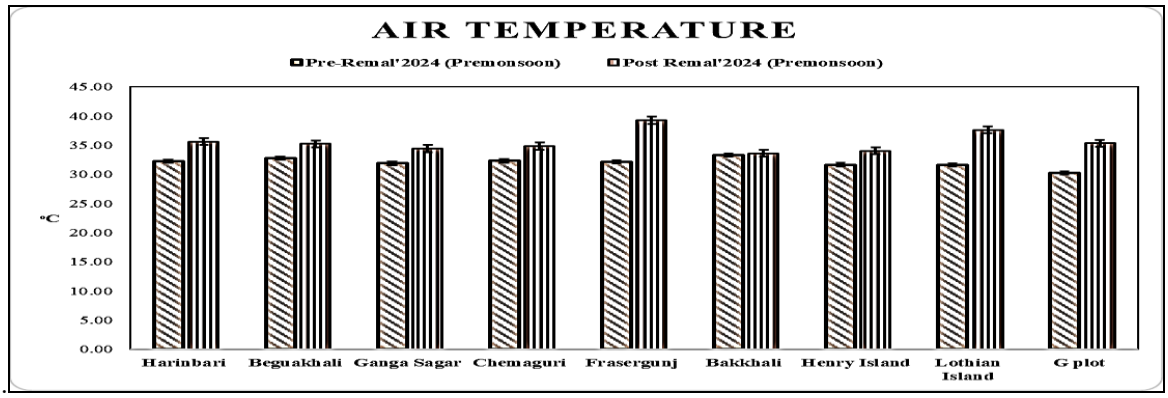

Fig. 5: Variations in ambient air temperature around the selected sites of sampling before and after the onset of Cyclone Remal

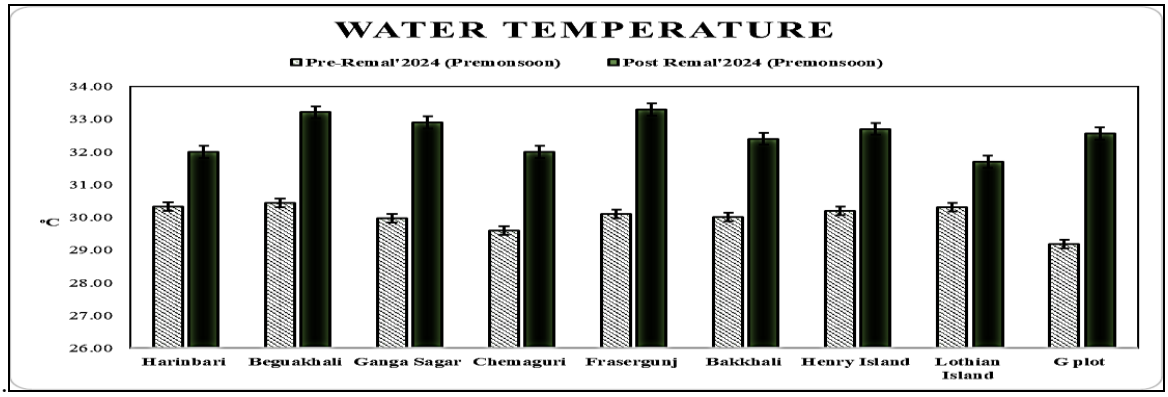

Fig. 6: Pre- and post 'Remal' fluctuations in ambient water temperature across the sampling stations of the selected study area.

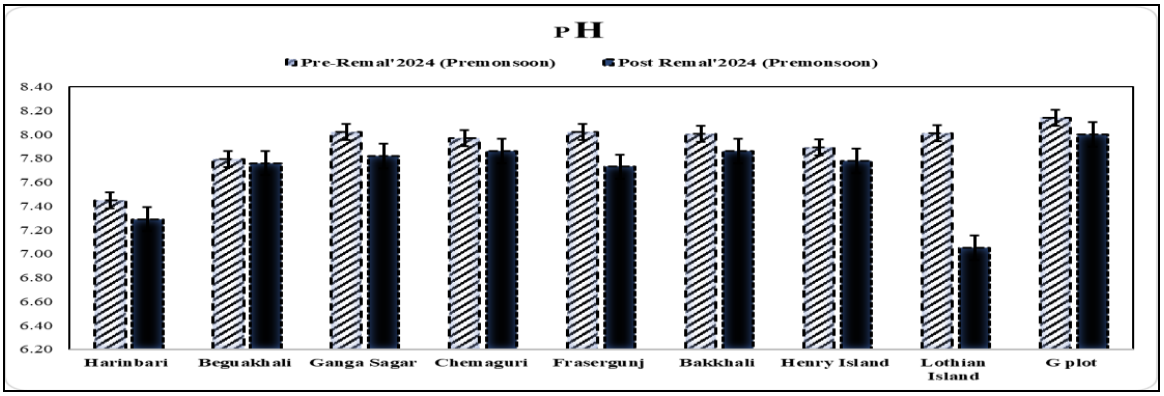

Fig. 7: Changes in the mean pH values along the selected sites of sampling, before and after the event of Cyclone Remal.

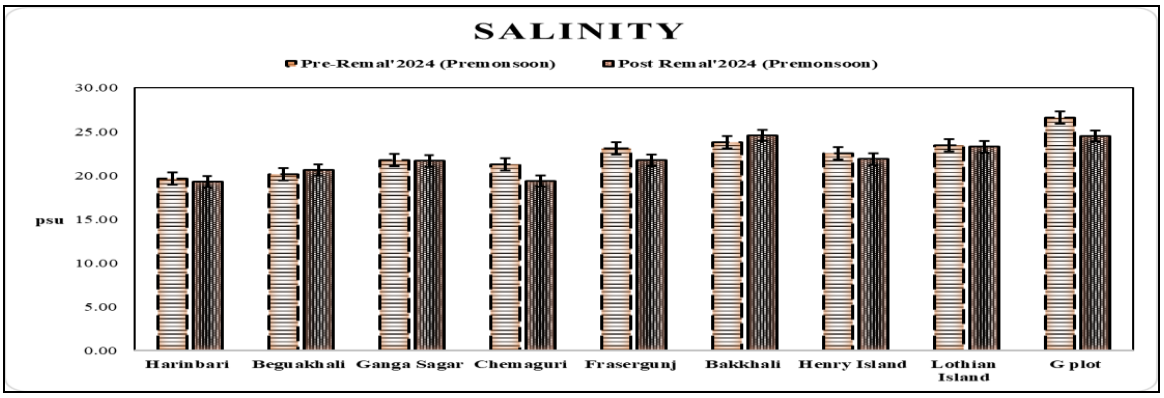

Fig. 8: Comparison in between the mean salinity values recorded before and after Cyclone Remal from the selected study area.

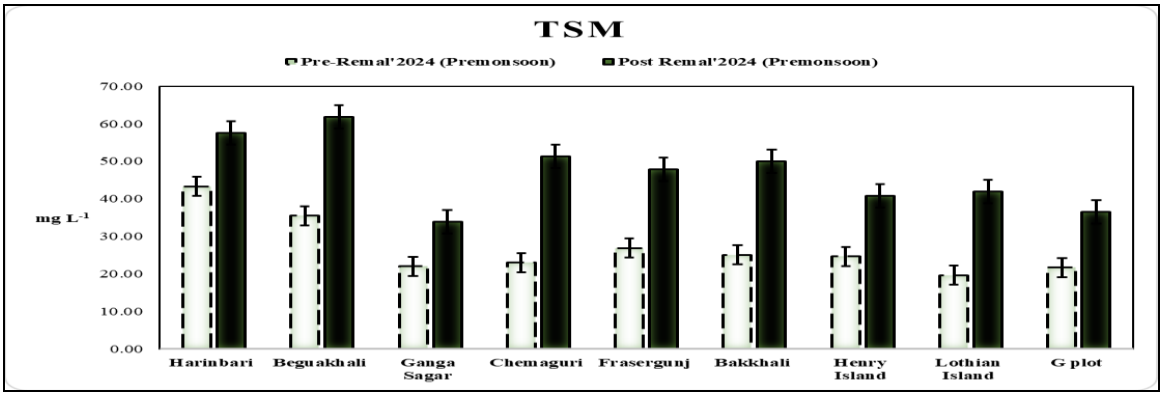

Fig. 9: Changes in the mean total suspended matter in the selected stations, during pre- and post 'Remal' month.

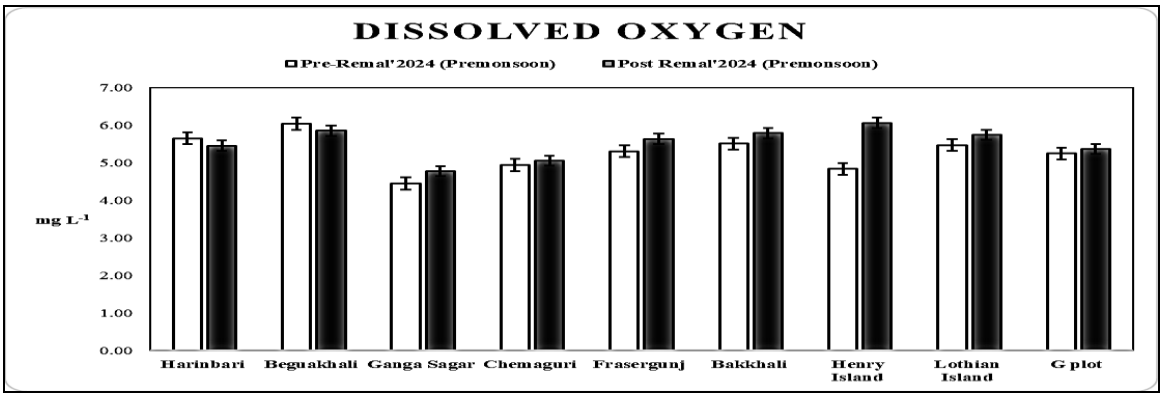

Fig. 10: Variation in dissolved oxygen contents, before and after Cyclone Remal, in the waters of the selected sites.

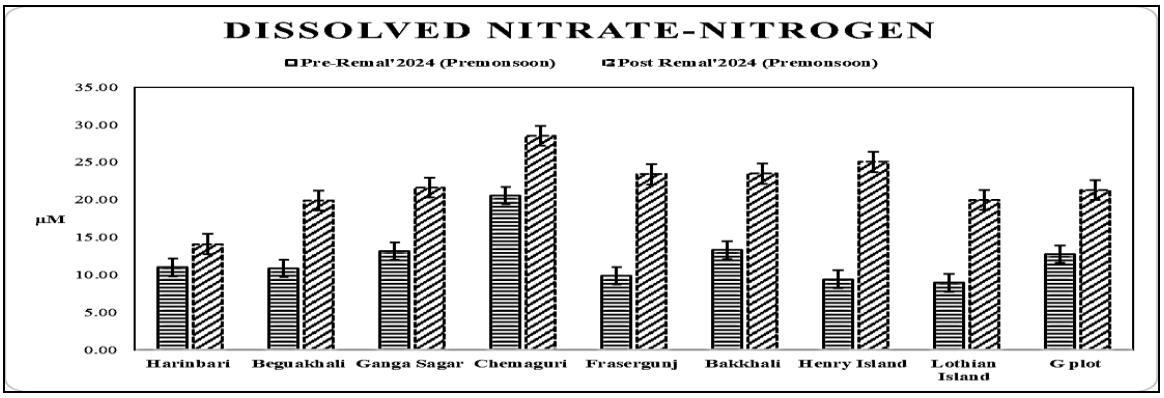

Fig. 11: Fluctuations in mean dissolved nitrate-nitrogen at the sampling sites before and after the event of Cyclone 'Remal'.

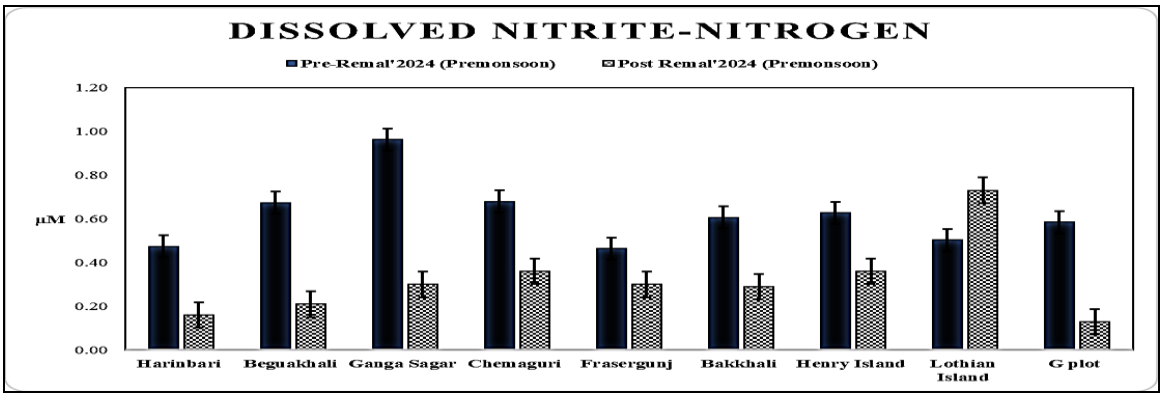

Fig. 12: Variation in mean dissolved nitrite-nitrogen contents in the study area, during pre- and post 'Remal' months.

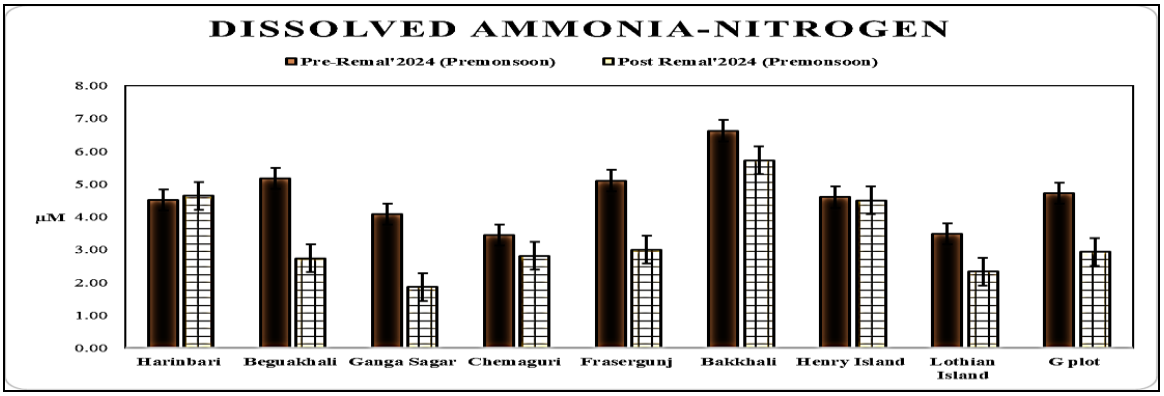

Fig. 13: Pre- and post 'Remal' changes in mean dissolved ammonia/ammonium-nitrogen across the study sites.

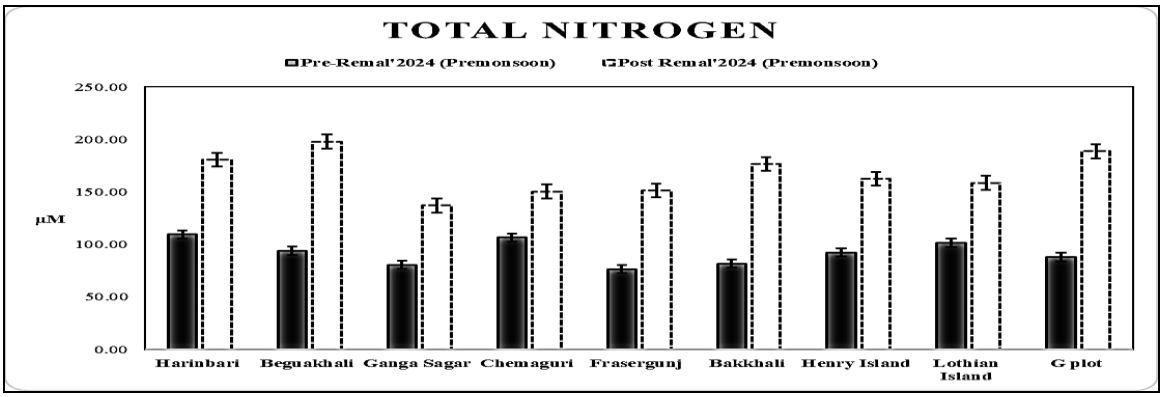

Fig. 14: Pre- and post 'Remal' changes in mean total nitrogen contents in the waters of the study area.

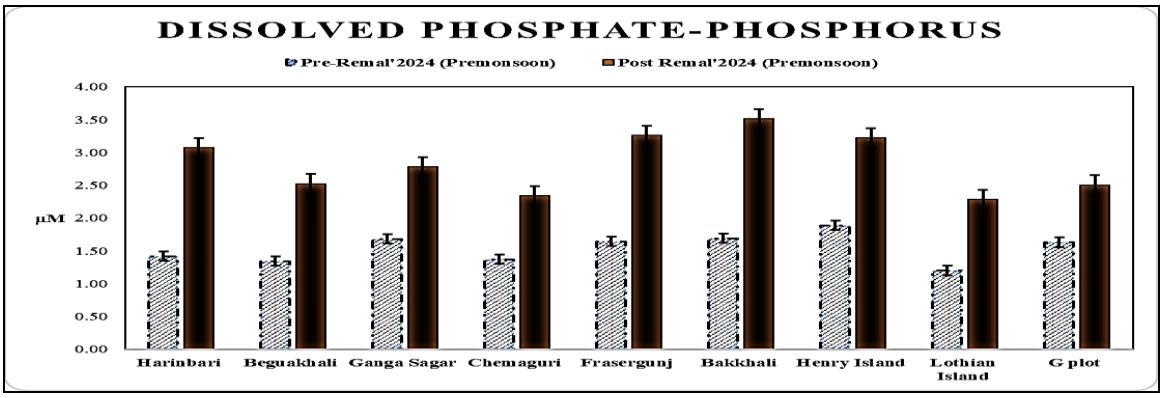

Fig. 15: Pre- and post 'Remal' changes in mean dissolved phosphate-phosphorus concentrations in the study region.

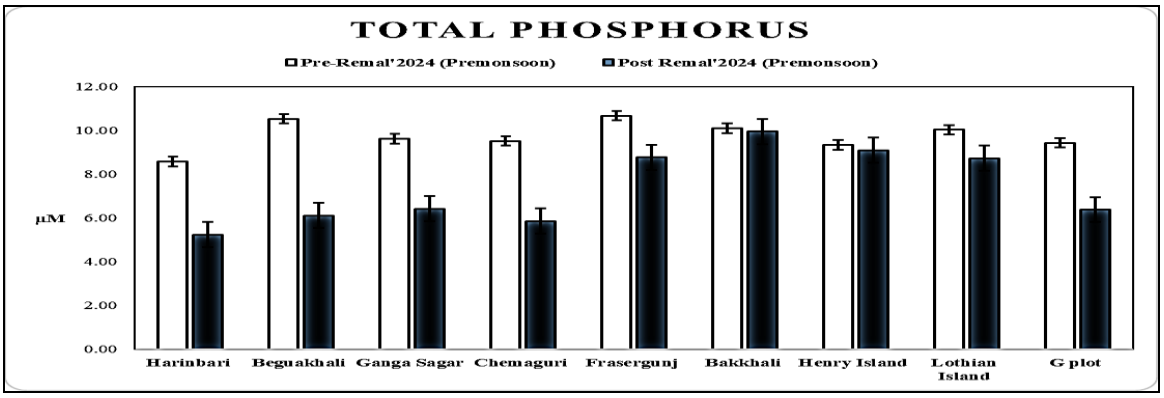

Fig. 16: Changes in the mean total phosphorus contents in the waters of the study area, both in the pre- and post 'Remal' months.

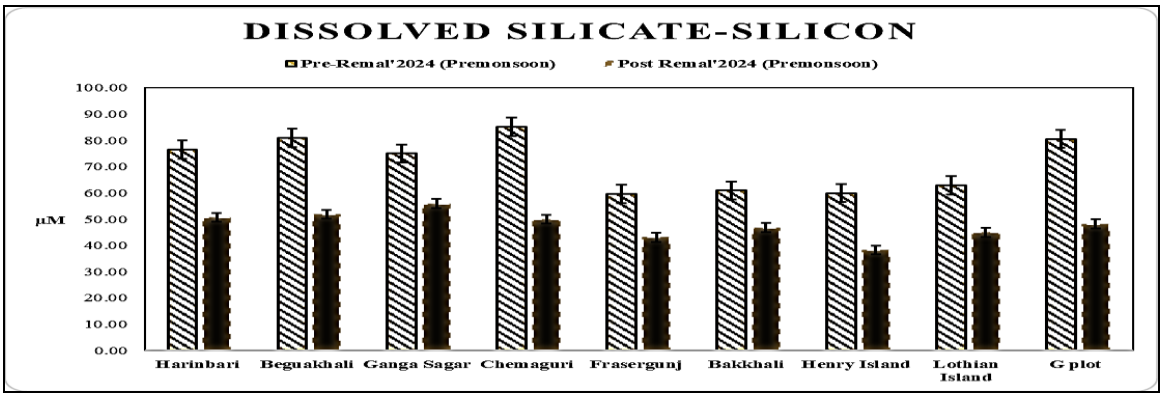

Fig. 17: Changes in mean dissolved silicate-silicon across the sampling sites before and after the event of Cyclone 'Remal'.

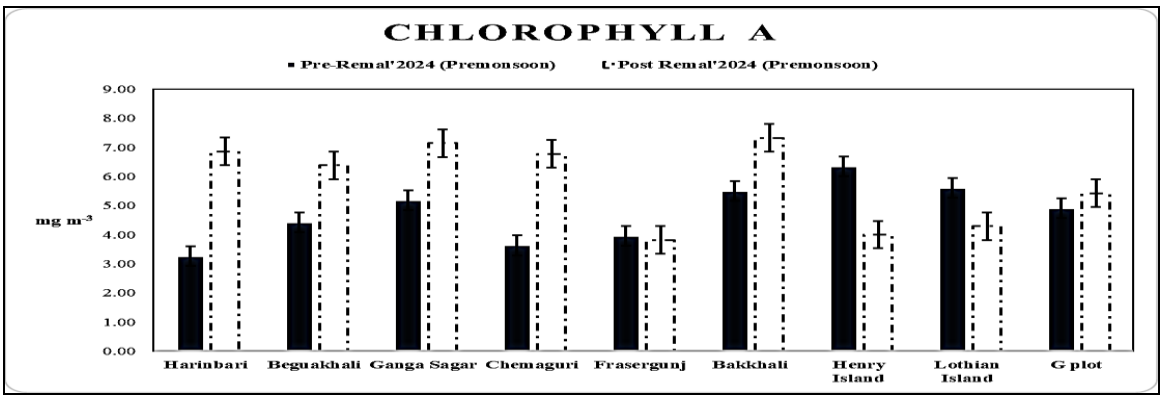

Fig. 18: Variation in chlorophyll *a* contents, before and after the event of Cyclone Remal, at the selected sites of sampling.

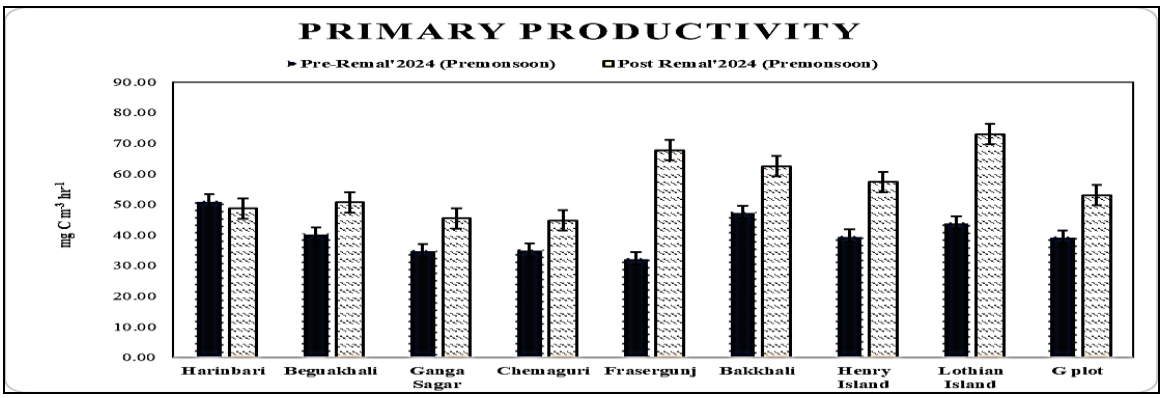

Fig. 19: Comparative primary productivity (GPP) recorded before and after Cyclone Remal across the selected study area.

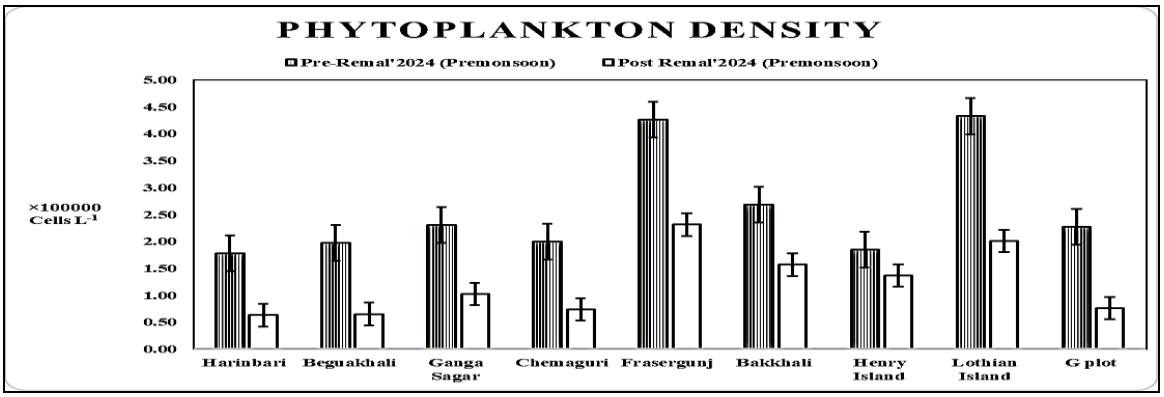

Fig. 20: The variation in the mean phytoplankton density across the selected sites before and after the Cyclone Remal.

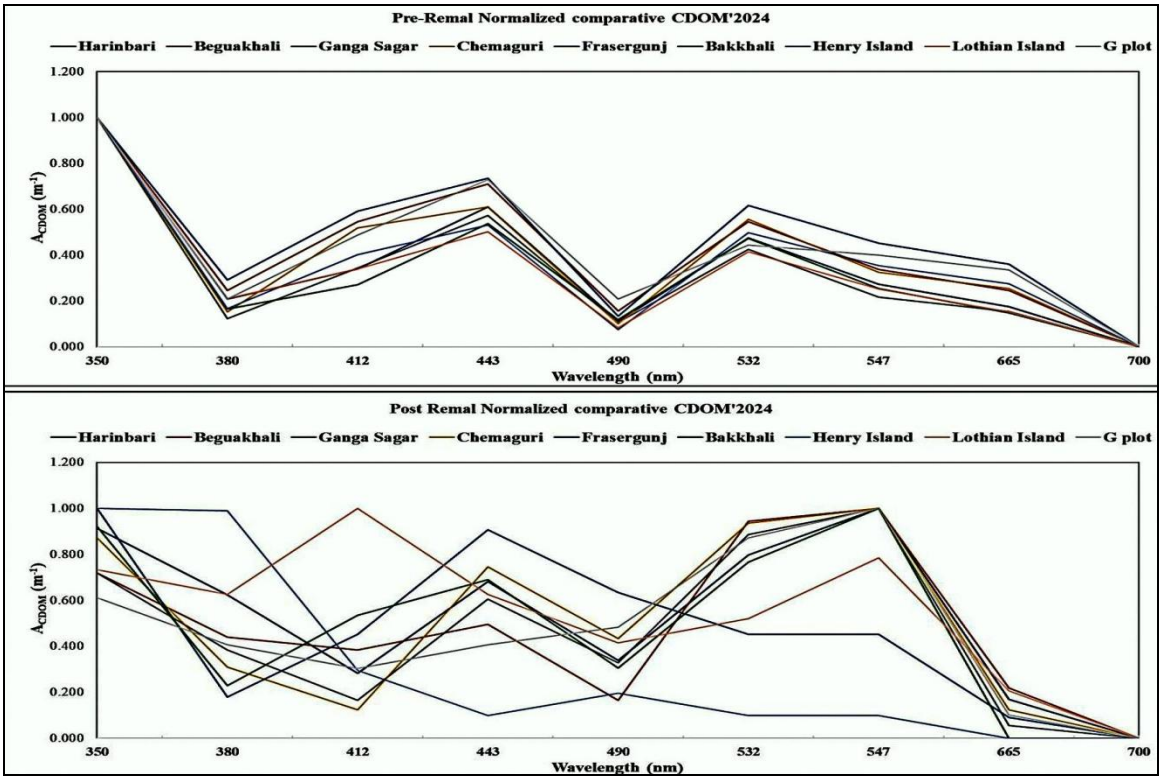

Fig. 21: Pre- and post 'Remal' comparative chart showing the variation in the mean chromophoric dissolved material in the selected sites encompassing the study area.

Table 1: Pre- and Post Cyclone Remal Sentinel 3 OCM derived mean Chl *a* and TSM data (±standard error) for the selected sampling sites within the study area (*in situ* and OCM Chl *a*: +0.6276; *in situ* and OCM TSM: +0.6389 at 95% level of significance).

Sites of Sampling	Latitude (°N)	Longitude (°E)	Pre-Remal Sentinel 3 OCM Chl *a* (mg m^{-3})	Post Remal Sentinel 3 OCM Chl *a* (mg m^{-3})	Pre-Remal Sentinel 3 OCM TSM (mg L^{-1})	Post Remal Sentinel 3 OCM TSM(mg L^{-1})
Harinbari	21.744	88.0616	14.40 ±2.31	16.41 ±1.06	52.80 ±9.02	77.93 ±12.05
Beguakhali	21.6573	88.0387	15.44 ±1.98	17.65 ±1.49	57.50 ±8.50	73.45 ±16.08
Ganga Sagar	21.6276	88.0739	17.31 ±3.02	19.28 ±2.05	58.97 ±6.31	80.82 ±19.33
Chemaguri	21.677	88.1604	14.95 ±1.52	17.34 ±1.66	69.72 ±8.12	94.66 ±20.14
Henry Island	21.5689	88.3075	18.83 ±1.88	13.51 ±1.35	64.78 ±10.66	100.14 ±18.47
Lothian Island	21.7069	88.3144	24.03 ±3.27	15.11 ±0.99	43.84 ±6.62	108.32 ±21.33
G plot	21.6948	88.4221	26.08 ±2.95	17.44 ±1.13	49.43 ±5.95	100.70 ±20.44
Frasergunj	21.5738	88.2302	12.40 ±1.08	14.93 ±1.04	54.38 ±7.15	120.45 ±23.30
Bakkhali	21.5507	88.2585	13.34 ±1.65	14.36 ±1.52	68.26 ±11.08	123.85 ±31.67

Table 2: Pre- and Post 'Remal' presence of Bacillariophycean microalgae and their respective frequency of occurrences in terms of the number of times a species has been observed among the selected sites; '+' denotes the number of time a species has been documented across the sampling stations; '-' denotes absence from within the collected phytoplankton assemblage respectively.

No.	Species	Habitat	Pre-Remal	Post Remal
1	***Actinocyclus curvatulus* Janisch**	**M***	+	-
2	***Actinocyclus normanii*(Gregory) Hustedt**	**M/F**	++	++
3	***Actinocyclus octonarius var. octonarius* Ehrenberg**	**M**	++	+
4	***Actinocyclus subtilis* (W.Gregory) Ralfs**	**M**	+	-
5	***Amphora ovalis* (Kützing) Kützing**	**M/F**	-	+
6	***Asterionella* cf. *glacialis* Castracane**	**M/F**	+++	++++++
7	***Asterionella japonica* Cleve**	**M/F**	++	+++++++
8	***Campylodiscus hibernicus* Ehrenberg**	**F**	+	-
9	***Cerataulina bergonii* Ostenfeld**	**M**	+++	++++
10	***Chaetoceros* cf. *didymus* Ehrenberg**	**M**	++	+++
11	***Chaetoceros curvisetus* Cleve**	**M**	-	+
12	***Chaetoceros lorenzianus* Grunow**	**M**	++	++++
13	***Cocconeis scutellum* Ehrenberg**	**M/F**	+++	++
14	***Coscinodiscus asteromphalus* Ehrenberg**	**M**	++++	++++
15	***Coscinodiscus centralis* Ehrenberg**	**M**	++++	++++
16	***Coscinodiscus concinnus* W.Smith**	**M**	++	++
17	***Coscinodiscus gigas* Ehrenberg**	**M**	-	++
18	***Coscinodiscus granii* Gough**	**M**	++	+++
19	***Coscinodiscus hyalinus* Grunow**	**M**	++	++
20	***Coscinodiscus lineatus* Ehrenberg**	**M/F**	+++++++++	+++++++
21	***Coscinodiscus marginatus* Ehrenberg**	**M**	+++++++++	+++++++
22	***Coscinodiscus oculus-iridis* (Ehrenberg) Ehrenberg**	**M**	+	+
23	***Coscinodiscus radiatus* Ehrenberg**	**M**	++++++++	++++++
24	***Cyclotella meneghiniana* Kützing**	**F**	+++++	+++++
25	***Cyclotella striata* (Kützing) Grunow**	**F**	+++++	+++++
26	***Ditylum brightwelii* (T.West) Grunow**	**M**	+++++++++	+++++++++

27	*Gyrosigma acuminatum* (Kützing) Rabenhorst	F	+	-
28	*Hobaniella longicruris* (Greville) P.A. Sims & D.M. Williams in Sims et al.	M	++++++	++++++
29	*Lioloma elongatum* (Grunow) Hasle	M	+	+
30	*Lioloma* cf. *delicatulum* (Cupp) Hasle	M	-	+
31	*Navicula socialis* T.C.Palmer	F	++++	++++
32	*Navicula* cf. *pelagica* Cleve	M	+++	+
33	*Navicula* cf. *salinarum* Grunow	B/F	-	+++
34	*Navicula transitans* Cleve	M	+	-
35	*Nitzschia sigma* (Kützing) W.Smith	F	+++++	+++++
36	*Nitzschia* cf. *sigmoidea* (Nitzsch) W.Smith	F	++	++
37	*Odontella sinensis* (Greville) Grunow	M	++++++	++++++
38	*Pinnularia directa* var. *directa* W. Smith	M	++	++
39	*Planktoniella blanda* (A.Schmidt) E.E.Syvertsen & G.R.Hasle	M	++	++
40	*Pleurosigma angulatum* (Queckett) W.Smith	B	+	-
41	*Pleurosigma* cf. *normanii* Ralfs	M/F	++	++
42	*Pleurosigma elongatum* W.Smith	M/B/F	++	++
43	*Pleurosigma formosum* W.Smith	F	++	+
44	*Skeletonema costatum* (Greville) Cleve	M	++++++	++++
45	*Sundstroemia setigera* (Brightwell) Medlin in Medlin et al.	M	++++	++++
46	*Synedra minutissima var.pelliculosa* Kützing	F	+++	-
47	*Thalassionema frauenfeldtii* (Grunow) Tempère & Peragallo	M	+++++++++	+++++++++
48	*Thalassionema nitzschioides* (Grunow) Mereschkowsky	M	++	+++
49	*Thalassiosira eccentrica* (Ehrenberg) Cleve	M	+++++	++++++

*M – Marine, B- Brackish, and F- Freshwater